

Carrier recombination dynamics in InGaN/GaN multiple quantum wells

Colin-N. Brosseau, Mathieu Perrin, Carlos Silva, and Richard Leonelli*

*Département de Physique and Regroupement Québécois sur les Matériaux de Pointe,
Université de Montréal, Case Postale 6128,
Succursale Centre-ville, Montréal,
Québec H3C 3J7, Canada*

(Dated: April 17, 2019)

Abstract

In spite their wide spread usage in light-emitting diodes and lasers, the recombination dynamics of photo-generated carriers in InGaN/GaN multiple quantum wells is still a subject of debate. To resolve this issue, we have measured the dynamics of such quantum wells over an unprecedented range in intensity. The dynamics are biphasic: at times shorter than 20 ns, they follow an exponential form, and a power law at times longer than 1 μ s. We propose a simple three-level model where a charge-separated state interplays with the radiative state through charge transfert following a tunneling mechanism. We show how the distribution of distance in charge-separated states controls the dynamics at long time. The results imply that charge recombination happens on nearly-isolated clusters of localisation centers.

PACS numbers: 78.47.-p, 78.47.Cd, 78.55.Cr, 78.67.De,

I. INTRODUCTION

$\text{In}_x\text{Ga}_{1-x}\text{N}/\text{GaN}$ heterostructures are essential in the production of optoelectronic devices, such as blue/ultraviolet lasers and light-emitting diodes, with external quantum efficiencies (EQE) approaching 75%.¹⁻³ The physical mechanisms that result in such high EQEs are still poorly understood, as high threading dislocation densities due to epitaxial growth on mismatched sapphire substrates should induce numerous non-radiative carrier recombination centers in these heterostructures.⁴⁻⁶ It is generally assumed that, because of the large electron and hole effective masses in InGaN, nanoscopic potential fluctuations induce a strong localization of the carrier wave function.^{7,8} Evidence for carrier localization in In-rich clusters^{9,10} and antilocalization near threading dislocations^{5,11,12} has been reported. Such a localization has a profound impact on carrier dynamics, which can be unraveled through time-resolved photoluminescence (PL) measurements. Indeed, the PL decay from InGaN/GaN heterostructures is highly non-exponential^{9,10,13-18} but a detailed understanding of these particular dynamics is still lacking. Early studies concluded that the recombination dynamics could be well described by a stretched exponential (SE).^{9,10,14-17} SEs are often observed in highly disordered materials,¹⁹ where they are assigned to the summation of monoexponential decays originating from individual localization centers with different exciton lifetimes.¹⁰

The quantum confined Stark effect (QCSE) has also been invoked to explain the carrier dynamics. It is induced in InGaN/GaN heterostructures by the large electric fields that result from the mechanical constraints inherently present in epitaxially grown nitrides combined with high piezoelectric coefficients. It leads to non-exponential recombination dynamics, redshift of the emission energy with time, and excitation density dependence on the emission energy.¹⁸ The QCSE is mostly observed in wide InGaN quantum wells (QW), as in QWs whose thickness is less than the exciton Bohr radius, where the e - h overlap integral is not modified by the presence of electric fields.²⁰

The localization of electrons and holes on separate sites has also been reported.^{11,21,22} The amphoteric character of the localization centers has led to proposals of a bidimensional donor-acceptor like recombination (2D-DAP) model where electrons and holes are localized on the opposite sides of the QWs. The 2D-DAP model was found to reproduce the PL decay dynamics of InGaN/GaN QWs over three decades in intensity.²¹

Recently, the non-exponential PL dynamics of ensembles of localized centers has been

linked to the PL intermittency, also called blinking, of individual centers whose emission is observed under continuous excitation conditions.^{23,24} Blinking is observed in a variety of systems such as colloidal QDs,^{23,25} Si nanocrystals,²⁴ InP and GaAs and is attributed to the formation of metastable, charge-separated (CS) dark states.

In this paper, we present ensemble measurements of the carrier recombination dynamics in InGaN/GaN QWs over a time window that allows us to follow the PL decay over six decades in intensity. We observe a previously unreported slowing down of the decay dynamics at times longer than 200 ns that cannot be explained by the SE, QCSE or 2D-DAP models. We propose a three-level recombination model involving a dark CS state to explain our results. We conclude that in thin InGaN/GaN QWs radiative recombination happens on nearly-isolated islands of agglomerated localisation centers.

II. EXPERIMENTAL DETAILS

InGaN/GaN samples were grown on c-plane sapphire substrates by metalorganic chemical vapor deposition. Five-period $\text{In}_x\text{Ga}_{1-x}\text{N}/\text{GaN}$ QWs were grown on $2\mu\text{m}$ n-GaN with a nominal In composition $x = 0.2$. The thickness of the GaN barriers and InGaN wells was respectively 14.0 and 2.0 nm. On top of the multiple QW structure, 14 nm of p-AlGaIn and 100 nm of p-GaN were deposited.

Time-resolved photoluminescence (TRPL) measurements were performed using a femtosecond Ti:sapphire laser system with a repetition rate of 1 kHz and a pulse duration of ≈ 40 fs. The second harmonic of the laser beam (KM Labs Dragon, $\lambda = 390$ nm), generated with a type-I β -BBO crystal, was focussed on the samples with an excitation density of about $3 \times 10^2 \text{ W cm}^{-2}$, corresponding to $6 \times 10^{12} \text{ photons cm}^{-2}$ per pulse. This excitation density is well within the linear regime of our samples. The samples were cooled to 9 K in a cold-finger liquid-helium continuous-flow cryostat. As the photon energy (3.18 eV) is lower than the low-temperature GaN band gap (3.5 eV), the carriers were photogenerated directly in the QWs. The PL signal was analyzed with a 0.3 m grating spectrometer and detected with a gated, intensified charge-coupled device (ICCD, Princeton Instrument PIMAX). The time evolution of the emission spectrum could be acquired with a temporal resolution of about 2 ns.

III. RESULTS AND DISCUSSION

Time-dependent photoluminescence (PL) spectra are presented in Fig. 1. Three distinct bands can be distinguished. Band A, at 2.81 eV, has a lifetime shorter than 4 ns. We attribute it to QW free-exciton recombination. Band B peaks at 2.74 eV. After a rapid energy shift for $t < 4$ ns, its shape and energy position remain constant with time. At times larger than $1 \mu\text{s}$, band C can be observed at 2.65 eV. The time-integrated PL spectrum is close to that of the time-resolved emission at 10 ns. As band B dominates the emission, we focus on its dynamics in what follows.

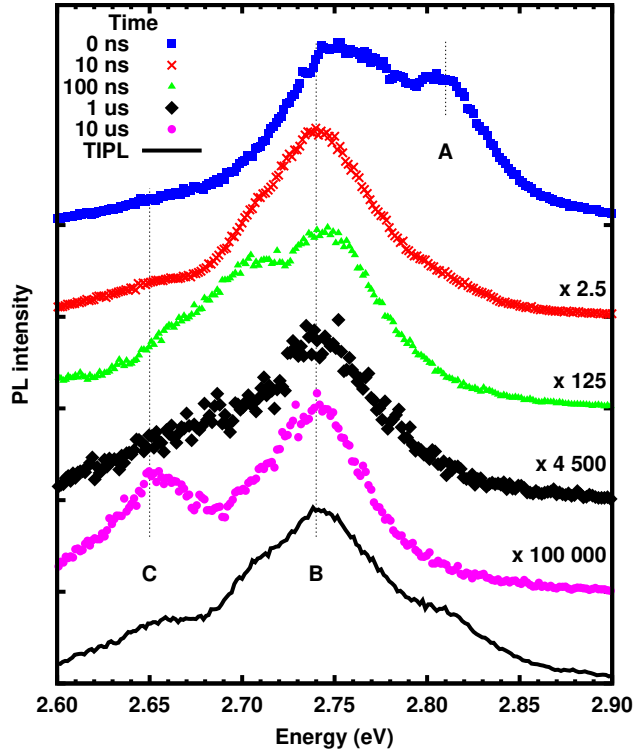


Figure 1: Time-resolved PL spectra. TIPL is the time-integrated emission. $E_{exc} = 3.18$ eV. Time resolution is 2 ns.

Figure 2 shows the decay of the emission from band B integrated from 2.73 to 2.76 eV. For times shorter than 30 ns, the intensity decreases rapidly and the dynamics are compatible with a SE. At longer times however, the dynamics slow down and tend to a power law $t^{-\alpha}$ with $\alpha = 1.3$ for $t > 200$ ns as can be seen on Fig. 2(a). The long-lived tail on the decay curve, which accounts for about 20% of the time integrated intensity, imposes stringent constraints on any dynamical model.

The absence of spectral shift with time, the invariance of the decay curve with excitation density, together with the small thickness of the InGaN QWs, rules out the presence of a QCSE in our samples.

The significant proportion of photons emitted in the long-lived tail (20%) implies that the power law is not caused by a rare occurrence of localization centers or impurities. In addition, because of the shape preservation of bands with time and the energy independence of decay dynamics, we interpret the decay dynamics as a single recombination channel. We then do not interpret the dynamics as the sum of exponential channels associated to a distribution of QDs.

Within the SE model, the PL intensity is assumed to follow

$$I(t) = I_0 \exp \left\{ -(\Gamma_{SE} t)^\beta \right\}. \quad (1)$$

As can be seen in Fig. 2(a), Eq. 1 reproduces our data with the parameters listed in Table I only for $t < 30$ ns, that is for less than two decades in intensity. Thus, in our samples, the SE model is at best a phenomenological description at short times.

The 2D-DAP model implies a decay dynamics that follow²¹

$$I(t) = 2\pi\gamma \int_0^\infty W(r) e^{-W(r)t} r dr \\ \times \exp \left\{ 2\pi\gamma \int_0^\infty (e^{-W(r)t} - 1) r dr \right\}, \quad (2)$$

where $W(r) = \Gamma_D e^{-r^2/a^2}$ represents the recombination rate for an electron-hole pair separated by a distance r , n is the majority carrier saturation density, and $\gamma = na^2$.

Figure 2 also shows the best fit of our data with Eq. 2. A good agreement is achieved for times up to about 200 ns with the optimized parameters listed in Table I. The value obtained for γ in our samples is close to that obtained by Morel *et al.* (Ref. 21). However, the 2D-DAP model fails to reproduce the decay slowing down observed at $t > 200$ ns.

Sher et al. introduced a three-level CS model to describe both PL blinking and non-exponential recombination dynamics in colloidal quantum dots.²³ It is based on the interplay between a *bright state* (1) that corresponds to an electron and a hole on the same localization center, and a *dark state* (2) where the carriers are spatially separated, as schematized in Fig. 3. Luminescence comes from transitions $1 \rightarrow 0$ with a rate constant Γ_{rad} , while transitions $1 \rightarrow 2$ occur with a rate constant Γ_{esc} . If one assumes that the back-transfer

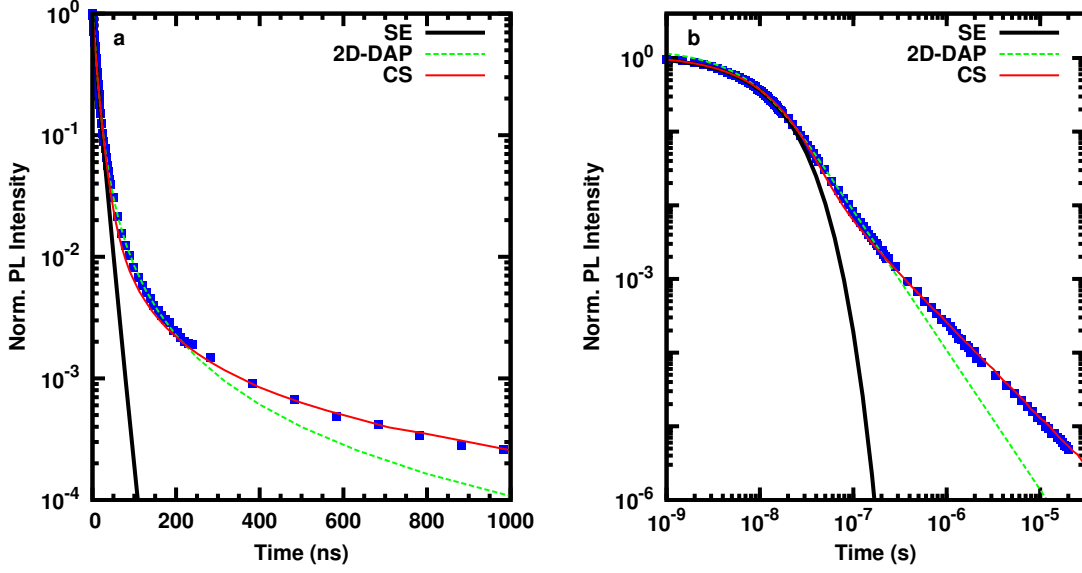


Figure 2: PL decay of band B. a) semilogarithmic plot; b) double logarithmic plot. The solid lines are the best fits using the SE, 2D-DAP, and CS models.

SE	2D-DAP
$\Gamma_{SE} = 1.22 \pm 0.08 \times 10^8 \text{ s}^{-1}$	$\Gamma_D = 1.1 \pm 0.1 \times 10^8 \text{ s}^{-1}$
$\beta = 0.83 \pm 0.09$	$\gamma = 0.28 \pm 0.02$
CS	
$\Gamma_{rad} = 8.4 \pm 0.6 \times 10^7 \text{ s}^{-1}$	
$\Gamma_{esc} = 1.1 \pm 0.2 \times 10^9 \text{ s}^{-1}$	
$\nu \equiv 2 \times 10^{13} \text{ s}^{-1}$	
$\mu = 0.3 \pm 0.01$	

Table I: Parameters of model fits to experimental data represented in Fig. 2.

$2 \rightarrow 1$ occurs by tunneling, the distribution of time spent in the dark state is

$$R(t) = \int_0^\infty f(r)k(r)e^{-k(r)t}dr, \quad (3)$$

where r is the distance between the carriers, $k(r) = \nu e^{-\eta r}$ is the tunneling rate, and $f(r)$ is the spatial distribution of charge separation.²⁶ Within the CS model, the PL intensity is given by

$$I(t) \propto \Gamma_{rad}x_1(t), \quad (4a)$$

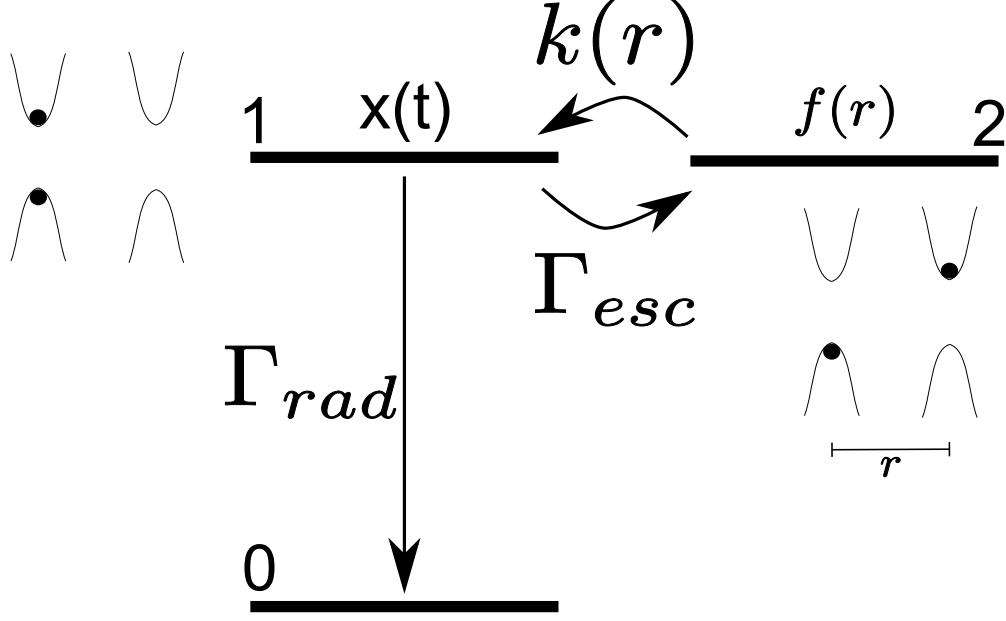


Figure 3: Charge separation recombination model (CS). State 1 corresponds to an electron and a hole on the same localization center. State 2 corresponds to carriers localized on different centers. Radiative transitions from state 1 to the ground state occur with rate constant Γ_{rad} and charge separation from state 1 to state 2 occur with a rate constant Γ_{esc} .

where x_1 is the population of state 1 and

$$\begin{aligned} \frac{dx_1(t)}{dt} = & -(\Gamma_{rad} + \Gamma_{esc})x_1(t) \\ & + \int_0^t \Gamma_{esc}x_1(t')R(t-t')dt'. \end{aligned} \quad (4b)$$

In the Laplace domain,

$$\hat{x}_1(s) = \left(s + \Gamma_{rad} + \Gamma_{esc}[1 - \hat{R}(s)] \right)^{-1}. \quad (5)$$

If an exponential spatial distribution is assumed, $f(r) = \epsilon e^{-\epsilon r}$, then

$$\hat{R}(s) = \mu \int_0^\infty \frac{e^{-(1+\mu)r}}{s/\nu + e^{-r}} dr, \quad (6)$$

where $\mu = \epsilon/\eta$. $\hat{R}(s)$ can be evaluated through numerical integration of Eq. 6 and $I(t)$ by an inverse Laplace transform of Eq. 5 using the Gaver-Stehfest algorithm.²⁷ Thus, the dynamics are controlled by μ .

The CS model predicts biphasic dynamics. At short times, the PL decays exponentially, $I(t) \propto e^{-\Gamma_{rad}t}$, while it follows a power law at long times, $I(t) \approx t^{-(1+\mu)}$. Equations 4b and

6 indicate that ν and Γ_{esc} cannot be determined independently. For a given tunnel attempt frequency ν , Γ_{esc} controls the strength of the long-time power law component with respect to the short-time exponential one.

As shown in Fig. 2, the CS model reproduces the experimental results throughout the entire range of the measurement with a vibronic-like attempt frequency²⁸ and the optimized parameters listed in Table I. However, excellent agreement can still be obtained over a wide range of attempt frequencies; our simulations show that $\Gamma_{esc} \gtrsim \Gamma_{esc}$ and $\nu > 10^{10} \text{ s}^{-1}$.

As the distribution of distances between charge-localization centers, $f(r)$, controls the recombination dynamics, we have tested that only a rapidly decreasing function, such an exponential, reproduce our results. This implies that carriers are confined in nearly isolated islands of grouped localization centers. Thus, one could hypothetize that many localization centers are in fact present in a single quantum dot.

Our results also allow to estimate the energy barrier between the *dark* and *brigth state*, E_{loc} as the back-transfer tunnel rate is $\eta = (8mE_{loc}\hbar^{-2})^{1/2}$. Given the composition of our wells, one can estimate the electronic effective mass as $m = 0.18 m_0$.²⁹ The fit of recombination dynamics gives $\mu = 0.31$. Assuming intra-dot carrier localization, the characteristic distance between localization centers is then $1/\epsilon \approx 3\text{-}6 \text{ nm}$.^{12,30,31} One then estimates $E_{loc} \approx 25\text{-}50 \text{ meV}$.

The CS model predicts PL blinking but this phenomenon has not been observed in our samples. We attribute this to the ensemble measurement we have performed. Nevertheless, blinking has already been observed in InGaN.^{32,33} As a test for our interpretation of the observed decay dynamics, one should be able to observe blinking on emission of single QD on our samples. In addition, distribution of *on* and *off* state duration would be related to μ .²³

The proposed model for recombination dynamics in InGaN seems to be valid in a variety of materials such as colloidal QDs²³ or polymer heterojunctions³⁴. This indicates that interaction of a charge-separated state with a radiative state plays a crucial role in the determination of long-time carriers recombinaition dynamics in disordered systems.

IV. CONCLUSION

Time-resolved PL had been measured on InGaN/GaN MQW over an unprecedented long time window. The dynamics show a slowing down at long times, following a power law. Current models cannot describe these peculiar dynamics. The TRPL can be well modelled by a simple three-level system with a *dark* charge-separated state and a *bright* radiative state. The interplay between the *dark* and *bright* states, through tunnel back-transfer, dominates the recombination dynamics at long times. Our results show that the distribution of distance between charge-localisation centers is a decreasing exponential. This implies that radiative recombination happens on nearly-isolated islands of agglomerated localisations centers.

Acknowledgments

CS acknowledges financial support from NSERC, CFI and The Canada Research Chair Program.

* Electronic address: richard.leonelli@umontreal.ca

¹ S. P. Shuji Nakamura and G. Fasol, *The blue laser diode* (Springer-Verlag, 2000).

² B. Gil, *Low-dimensional nitride semiconductors* (Oxford Univ. Press, 2002).

³ Y. Narukawa, M. Sano, M. Ichikawa, S. Minato, T. Sakamoto, T. Yamada, and T. Mukai, Jpn. J. Appl. Phys. Part 2 **46**, L963 (2007).

⁴ S. J. Rosner, E. C. Carr, M. J. Ludowise, G. Girolami, and H. I. Erikson, Appl. Phys. Lett. **70**, 420 (1997).

⁵ A. Kaneta, M. Funato, and Y. Kawakami, Phys. Rev. B **78**, 125317 (2008).

⁶ T. Sugahara, H. Sato, M. Hao, Y. Naoi, S. Kurai, S. Tottori, K. Yamashita, K. Nishino, L. T. Romano, and S. Sakai, Jpn. J. Appl. Phys. **37**, L398 (1998).

⁷ H. Schömig, S. Halm, A. Forchel, G. Bacher, J. Off, and F. Scholz, Phys. Rev. Lett. **92**, 106802 (2004).

⁸ D. M. Graham, A. Soltani-Vala, P. Dawson, M. J. Godfrey, T. M. Smeeton, J. S. Barnard, M. J. Kappers, C. J. Humphreys, and E. J. Thrush, J. Appl. Phys. **97**, 103508 (2005).

- ⁹ I. L. Krestnikov, N. N. Ledentsov, A. Hoffmann, D. Bimberg, A. V. Sakharov, W. V. Lundin, A. F. Tsatsul'nikov, A. S. Usikov, Zh. I. Alferov, Yu. G. Musikhin, and D. Gerthsen, *Phys. Rev. B* **66**, 155310 (2002).
- ¹⁰ T. Bartel, M. Dworzak, M. Strassburg, A. Hoffmann, A. Strittmatter, and D. Bimberg, *Appl. Phys. Lett.* **85**, 1946 (2004).
- ¹¹ A. Hangleiter, C. Netzel, D. Fuhrmann, F. Hitzel, L. Hoffmann, H. Bremers, U. Rossow, G. Ade, and P. Hinze, *Philosophical Magazine* **87**, 2041 (2007).
- ¹² Y. Narukawa, Y. Kawakami, M. Funato, S. Fujita, S. Fujita, and S. Nakamura, *Appl. Phys. Lett.* **70**, 981 (1997).
- ¹³ Y. Sun, Y.-H. Cho, E.-K. Suh, H. J. Lee, R. J. Choi, and Y. B. Hahn, *Appl. Phys. Lett.* **84**, 49 (2004).
- ¹⁴ M. Pophristic, F. H. Long, C. Tran, I. T. Ferguson, and R. F. Karliceck, Jr., *J. Appl. Phys.* **86**, 1114 (1999).
- ¹⁵ SF. Chichibu, T. Onuma, T. Sota, S. P. DenBaars, S. Nakamura, T. Kitamura, Y. Ishida, and H. Okumura, *J. Appl. Phys.* **93**, 2051 (2003).
- ¹⁶ T. Onuma, A. Chakraborty, B. A. Haskell, S. Keller, S. P. DenBaars, J. S. Speck, S. Nakamura, U. K. Mishra, T. Sota, and S. F. Chichibu, *Appl. Phys. Lett.* **86**, 151918 (2005).
- ¹⁷ S.-Y. Kwon, H. J. Kim, E. Yoon, Y. Jang, K.-J. Yee, D. Lee, S.-H. Park, D.-Y. Park, H. Cheong, F. Rol, and L. S. Dang, *J. Appl. Phys.* **103**, 063509 (2008).
- ¹⁸ P. Lefebvre, S. Kalliakos, T. Bretagnon, P. Valvin, T. Taliercio, B. Gil, N. Grandjean, and J. Massies, *Phys. Rev. B* **69**, 035307 (2004).
- ¹⁹ H. Scher, M. F. Shlesinger, and J. T. Bender, *Phys. Today* **26**, 24 (1991).
- ²⁰ P. Bigenwald, P. Lefebvre, T. bretagnon, and B. Gil, *phys. stat. sol. (a)* **216**, 371 (1999).
- ²¹ A. Morel, P. Lefebvre, S. Kalliakos, T. Taliercio, T. Bretagnon, and B. Gil, *Phys. Rev. B* **68**, 045331 (2003).
- ²² S. Kalliakos, X. B. Zhang, T. Taliercio, P. Lefebvre, B. Gil, N. Grandjean, B. Damilano, and J. Massies, *Appl. Phys. Lett.* **80**, 428 (2002).
- ²³ P. H. Sher, J. M. Smith, P. A. Dalgarno, R. J. Warburton, X. Chen, P. J. Dobson, S. M. Daniels, N. L. Pickett, and P. O'Brien, *Appl. Phys. Lett.* **92**, 101111 (2008).
- ²⁴ K. Dunn, J. Derr, T. Johnston, M. Chaker, and F. Rosei, *Phys. Rev. B* **80**, 035330 (2009).
- ²⁵ M. Nirmal, B. O. Dabbousi, M. G. Bawendi, J. J. Macklin, J. K. Trautman, T. D. Harris, and

- L. E. Brus, *Nature* **383**, 802 (1996).
- ²⁶ M. Tachiya and K. Seki, *Appl. Phys. Lett.* **94**, 081104 (2009).
- ²⁷ H. Stehfest, *Commun. ACM* **13**, 47 (1970).
- ²⁸ A. C. Morteani, A. S. Dhoot, J.-S. Kim, C. Silva, N. C. Greenham, C. Murphy, E. Moons, S. CinÁá, J. H. Burroughes, and R. H. Friend, *Advanced Materials* **15**, 1708 (2003).
- ²⁹ P. Rinke, M. Winkelnkemper, A. Qteish, D. Bimberg, J. Neugebauer, and M. Scheffler, *Phys. Rev. B* **77**, 075202 (2008).
- ³⁰ S. Chichibu, T. Azuhata, T. Sota, and S. Nakamura, *Appl. Phys. Lett.* **69**, 4188 (1996).
- ³¹ I. P. Soshnikov, V. V. Lundin, A. S. Usikov, I. P. Kalmykova, N. N. Ledentsov, A. Rosenauer, B. Neubauer, and D. Gerthsen, *Semiconductors* **34**, 621 (2000).
- ³² R. Micheletto, M. Abiko, A. Kaneta, Y. Kawakami, Y. Narukawa, and T. Mukai, *Appl. Phys. Lett.* **88**, 061118 (2006).
- ³³ T. Aoki, Y. Nishikawa, and M. Kuwata-Gonokami, *Appl. Phys. Lett.* **78**, 1065 (2001).
- ³⁴ S. Gélinas, C.-N. Brosseau, O. Paré-Labrosse, I. A. Howard, K. R. Kirov, R. H. Friend, R. Leonelli, and C. Silva, submitted to *Advanced Materials*.